Stability analysis of a non-singular fractional-order covid-19 model with nonlinear incidence and treatment rate

Physica Scripta

PAPER

Stability analysis of a non-singular fractional-order covid-19 model with nonlinear incidence and treatment rate

Hardik Joshi[1], **Mehmet Yavuz**[2,3,*], **Stuart Townley**[3] **and Brajesh Kumar Jha**[4]

[1] Department of Mathematics, LJ Institute of Engineering and Technology, LJ University, Ahmedabad-382210, Gujarat, India
[2] Department of Mathematics and Computer Sciences, Necmettin Erbakan University, Konya 42090, Turkey
[3] Centre for Environmental Mathematics, Faculty of Environment, Science and Economy, University of Exeter, TR10 9FE, United Kingdom
[4] Department of Mathematics, School of Technology, Pandit Deendayal Energy University, Gandhinagar 382007, India
[*] Author to whom any correspondence should be addressed.

E-mail: hardik.joshi8185@gmail.com, mehmetyavuz@erbakan.edu.tr, S.B.Townley@exeter.ac.uk **and** brajeshjha2881@gmail.com

Keywords: SIR model, Beddington-DeAngelis infection rate, Holling type-II treatment rate, local and global stability, Mittag-Leffler law

OPEN ACCESS

RECEIVED
18 December 2022

REVISED
9 February 2023

ACCEPTED FOR PUBLICATION
23 February 2023

PUBLISHED
16 March 2023

Abstract

In this paper, a non-singular SIR model with the Mittag-Leffler law is proposed. The nonlinear Beddington-DeAngelis infection rate and Holling type II treatment rate are used. The qualitative properties of the SIR model are discussed in detail. The local and global stability of the model are analyzed. Moreover, some conditions are developed to guarantee local and global asymptotic stability. Finally, numerical simulations are provided to support the theoretical results and used to analyze the impact of face masks, social distancing, quarantine, lockdown, immigration, treatment rate of the disease, and limitation in treatment resources on COVID-19. The graphical results show that face masks, social distancing, quarantine, lockdown, immigration, and effective treatment rates significantly reduce the infected population over time. In contrast, limitation in the availability of treatment raises the infected population.

1. Introduction

COVID-19 affects the human population worldwide and is caused by the SARS-COV-2 virus. The extent of COVID-19 is reduced in a few countries due to the development of vaccination, wearing of proper face masks, frequently hand washing, maintaining social distancing, avoiding public and crowded places, advertisements, adequate medical facilities, and following the guideline given by the World Health Organization (WHO) and national governments. But still, significant new cases of COVID-19 are registered in many regions across the world.

Mathematical models in epidemiology are great tools that can help us to understand the transmission dynamics of COVID-19 Ahmad *et al* (2022), Allegretti *et al* (2021), Biswas *et al* (2020), Erturk and Kumar (2020), Gao *et al* (2020), Kumar *et al* (2020), Naik *et al* (2020a, 2020b), Rajagopal *et al* (2020), Sene (2020), Kumar and Erturk (2021), Naik *et al* (2021), Safare *et al* (2021), Sitthiwirattham *et al* (2021), Özköse *et al* (2022), Özköse and Yavuz (2022), Karim *et al* (2022), Kurmi and Chouhan (2022), Pandey *et al* (2022), Guo and Li (2022), Haq *et al* (2022), Li and Guo (2022a, 2022b), Pérez and Oluyori (2022), Swati (2022), Joshi *et al* (2023). It captures all the scenarios in a very compact form and by proper analysis of these models show, for example, (I) how the disease spreads worldwide, (II) how much population is affected, (III) how to constrain COVID-19. A simple model of COVID-19 is an SIR model with a bilinear incidence rate. It includes the basic three-compartment classes, namely the susceptible (S), infected (I), and recovered (R) classes. The variety of approaches to treating COVID-19 leads to a need for new compartment classes so as to understand, for example, the effects of quarantine Mishra *et al* (2020), Memon *et al* (2021), Nabi *et al* (2021), lockdown Atangana (2020), Sun *et al* (2020), face masks Srivastav *et al* (2021), social distancing Yasir and Liu (2021), vaccination Yavuz *et al* (2021) and immigration Ma *et al* (2022). The use of compartment classes in epidemiological modeling provides great

freedom to analyze infectious diseases from diverse angles. However, extending the classes, and so the complexity of the model, makes the qualitative analysis more laborious, and computational costs are increased.

So far, there have been many attempts to study the effects of face masks, social distancing, quarantine, lockdown, immigration, treatment rate of disease, and limitation in the treatment of COVID-19 by using elaborate models with five to eight compartments classes. We proposed an SIR model with nonlinear infection and treatment rates to overcome this increased complexity.

Infection and treatment rates play a vital role in reducing the dimension of the COVID-19 model, so it turns to enable better analysis. The WHO declared COVID-19 as a global pandemic in march 2020 WHO (2020). In this situation, it is unreasonable to choose a bilinear infection rate to formulate the COVID-19 model. Hence to overcome this disadvantage we chose the nonlinear infection rate introduced by Beddington and DeAngelis Beddington (1975), DeAngelis *et al* (1975). The Beddington-DeAngelis infection rate is defined as

$$f(S, I) = \frac{\beta SI}{1 + \xi_1 S + \xi_2 I}, \ \beta > 0, \ \xi_1 \geqslant 0, \ \xi_2 \geqslant 0, \tag{1}$$

where β is the transmission rate of disease, ξ_1 is a measure of inhibition for the susceptible population, and ξ_2 is a measure of inhibition for the infected population.

The common population-wide effort to reduce transmission of COVID-19 is to impose a lockdown. One prevention measure used by susceptible populations includes proper use of face masks and social distancing to reduce disease transmission. Prevention measures taken by the infected population include quarantine and self-isolation so as to reduce transmission or aid recovery from the disease. In our model, β is used to capture the impact of lockdown, ξ_1 is used to capture the impact of face masks and social distancing, and ξ_2 is used to represent the impact of quarantining.

The selection of treatment rate is also very crucial in formulating a COVID-19 model. During the initial phase of COVID-19, there were multiple crises in accessing hospitals, obtaining vaccines, securing oxygen cylinders, and other medical resources. Over time, the situation improved slowly in terms of the availability of hospitals, vaccines, and other medical facilities. To describe this situation, we chose the Holling type-II treatment due to its ability to capture this scenario. Zhou and Fan introduced the Holling type-II treatment rate and defined it as Zhou and Fan (2012)

$$g(I) = \frac{\varphi I(t)}{1 + \rho I(t)}, \ \varphi \geqslant 0, \ I \geqslant 0, \ \rho \geqslant 0, \tag{2}$$

where φ is the treatment rate of the disease, and ρ is the limitation in treatment availability.

To the best of our knowledge, SIR models with a Beddington-DeAngelis infection rate, a Holling type-II treatment rate with Mittag-Leffler law have not been used to examine the effects of face masks, social distancing, quarantine, lockdown, immigration, treatment rate of disease, and limitation in treatment resources on COVID-19.

The manuscript is organized as follows: in section 2, we provide a necessary definition of the non-local and non-singular Atangana-Baleanu operator. In section 3, the SIR model with the Mittag-Leffler law is formulated. The qualitative properties and local and global asymptotic stability of the model, under some conditions, are discussed in section 4. In section 6, the numerical results are discussed. Finally, some conclusions are provided in section 7.

2. Preliminaries

In this section, we provide a necessary definition of fractional calculus that is used in the development and numerical simulation of the model Atangana and Baleanu (2016).

Definition 1. Let $\alpha \in (0, 1]$ and $f \in H^1(a, b), \ a < b$ be any function. Then the Atangana-Baleanu Caputo (ABC) derivative is defined as

$${}_0^{ABC}D_t^{\alpha} f(t) = \frac{B(\alpha)}{1 - \alpha} \int_0^t f'(x) E_{\alpha}\left[-\alpha \frac{(t - x)^{\alpha}}{1 - \alpha} \right] dx, \tag{3}$$

where $B(\alpha) = 1 - \alpha + \frac{\alpha}{\Gamma(a)}$ is a normalization function satisfying $B(0) = B(1) = 1$.

Definition 2. Let $\alpha \in (0, 1]$ and $f \in H^1(a, b), \ a < b$ be any function. Then the Atangana-Baleanu derivative in the Riemann-Liouville sense is defined as

$${}_0^{ABR}D_t^{\alpha} f(t) = \frac{B(\alpha)}{1 - \alpha} \frac{d}{dt} \int_0^t f(x) E_{\alpha}\left[-\alpha \frac{(t - x)^{\alpha}}{1 - \alpha} \right] dx. \tag{4}$$

Table 1. Description of biological parameters of the SIR model.

Parameter	Description of parameter
S	Susceptible populations
I	Infected populations
R	Recovered populations
Λ	New recruitment rate of susceptible populations due to immigration
β	Disease transmission rate
ξ_1	Rate of social distancing and wearing face masks
ξ_2	Quarantine rate
μ	Natural death rate
η	Infection death rate
γ	Natural recovery rate
φ	Treatment rate
ρ	Limitation rate in treatment capacity

Definition 3. The fractional integral in the Atangana-Baleanu sense is defined as

$$ {}^{AB}_{0}I^{\alpha}_{t} f(t) = \frac{1-\alpha}{B(\alpha)} f(t) + \frac{\alpha}{B(\alpha)} ({}^{RL}_{0}I^{\alpha}_{t} f)(t), \tag{5} $$

where ${}^{RL}_{0}I^{\alpha}_{t}$ is the Riemann-Liouville fractional integral.

Definition 4. The Laplace transform of the ABC derivative of a function $f(t)$ of order $\alpha > 0$ is defined as

$$ \mathcal{L}\{{}^{ABC}_{a}D^{\alpha}_{t} f(t)\}(s) = B(\alpha)\frac{s^{\alpha}\mathcal{L}\{f(t)\}(s) - s^{\alpha-1}f(0)}{(1-\alpha)s^{\alpha} + \alpha}. \tag{6} $$

3. Formulation of a mathematical model

Here, we consider an SIR model with Beddington-DeAngelis type infection rate and Holling type II treatment rate. The basic SIR model is described by the following system of differential equations.

$$ \begin{aligned} \frac{dS(t)}{dt} &= \Lambda - \frac{\beta S(t) I(t)}{1 + \xi_1 S(t) + \xi_2 I(t)} - \mu S(t), \\ \frac{dI(t)}{dt} &= \frac{\beta S(t) I(t)}{1 + \xi_1 S(t) + \xi_2 I(t)} - \mu I(t) - \eta I(t) - \gamma I(t) - \frac{\varphi I(t)}{1 + \rho I(t)}, \\ \frac{dR(t)}{dt} &= \gamma I(t) - \mu R(t) + \frac{\varphi I(t)}{1 + \rho I(t)}, \end{aligned} \tag{7} $$

with the given initial conditions $S(0) = S_0 \geqslant 0$, $I(0) = I_0 \geqslant 0$, and $R(0) = R_0 \geqslant 0$. The variables, parameters, and biological interpretation are given in table 1.

The susceptible populations in compartment models use their memory to prevent infection. Due to this reason, the fractional-order model achieved high attention in modeling a biological process. Hence we convert the classical model (7) into the fractional-order one to enhance the accuracy of the model Podlubny (1998), Magin (2004), Hanert *et al* (2011), Baleanu *et al* (2012), Joshi and Jha (2018, 2021a, 2021b, 2022). However, there are many other definitions of the fractional derivative available to deal with the memory effect. The Caputo derivative is well known and widely used in the literature for the development of a fractional order model. The authors in Swati (2022) have studied the Caputo fractional order SIR model with BeddingtonDeAngelis incidence and Holling type II treatment rate. But the Caputo derivative consists of a singular power kernel that leads to many complexities in the problem. To overcome this disadvantage, we consider the ABC fractional derivative that consists of a non-singular Mittag-Leffler kernel Atangana and Baleanu (2016). Thus the classical model (7) is transformed to the fractional-order in the ABC sense as

$$ \begin{aligned} {}^{ABC}_{0}D^{\alpha}_{t} S(t) &= \Lambda - \frac{\beta S(t) I(t)}{1 + \xi_1 S(t) + \xi_2 I(t)} - \mu S(t), \\ {}^{ABC}_{0}D^{\alpha}_{t} I(t) &= \frac{\beta S(t) I(t)}{1 + \xi_1 S(t) + \xi_2 I(t)} - \mu I(t) - \eta I(t) - \gamma I(t) - \frac{\varphi I(t)}{1 + \rho I(t)}, \\ {}^{ABC}_{0}D^{\alpha}_{t} R(t) &= \gamma I(t) - \mu R(t) + \frac{\varphi I(t)}{1 + \rho I(t)}, \end{aligned} \tag{8} $$

where $S(0) = S_0$, $I(0) = I_0$, and $R(0) = R_0$.

4. Model analysis

In the epidemiological model, we must ensure that the solution is non-negative and bounded for all time. Let $\Omega = \{(S, I, R) \in R_+^3: S, I, R \in R^+\}$ be the required region.

Lemma 1. *Let $f(t) \in C[a, b]$ and suppose ${}_0^{ABC}D_t^{\alpha} f(t) \in C[a, b]$ where $\alpha \in (0, 1]$. Then the generalized mean value theorem states that*

$$f(t) = f(a) + \frac{1}{\Gamma(\alpha)} {}_0^{ABC}D_t^{\alpha} f(s)(t-a)^{\alpha}, \tag{9}$$

where $0 \leqslant s \leqslant t$.

Let $\alpha \in (0, 1]$, $f(t) \in C[0, b]$ and ${}_0^{ABC}D_t^{\alpha} f(t) \in C(0, b]$. It is clear from lemma 1 that if ${}_0^{ABC}D_t^{\alpha} f(t) \geqslant 0, \ \forall t \in (0, b]$, then the function $f(t)$ increases whilst if ${}_0^{ABC}D_t^{\alpha} f(t) \leqslant 0, \ \forall t \in (0, b]$, then the function $f(t)$ decreases.

Lemma 2. *Podlubny (1998), Magin (2004), Baleanu* et al *(2012) Let $\mu > 0$, $\gamma > 0$, and $p \in C$. Define $f(t) = t^{\gamma-1}E_{\mu,\gamma}(\pm pt^{\mu})$, where $E_{\mu,\gamma}(\cdot)$ represents the two-parameter Mittag-Leffler function. The Laplace transform of a function* f (t) *is defined as $L\{f(t)\} = \frac{s^{\mu-\gamma}}{s^{\mu} \mp p}$.*

Theorem 3. *Every solution of (8) remains in the region Ω. Moreover, the solutions are positively invariant and bounded.*

Proof. First, we show that the solutions of model (8) are positively invariant in the region Ω. We have

$$\begin{aligned} &{}_0^{ABC}D_t^{\alpha} S(t)|_{S=0} = \Lambda > 0, \\ &{}_0^{ABC}D_t^{\alpha} I(t)|_{I=0} = 0, \\ &{}_0^{ABC}D_t^{\alpha} R(t)|_{R=0} = \gamma I(t) + \frac{\varphi I(t)}{1 + \rho I(t)} \geqslant 0. \end{aligned} \tag{10}$$

Hence for all $t \geqslant 0$, and from lemma 1, we concluded that all the solutions of the model (8) are positively invariant. Next, we prove the boundedness of the model (8) with the framework of equation (3).

By summing up all the equations of the model (8), we have

$${}_0^{ABC}D_t^{\alpha} N(t) = \Lambda - \mu N(t) - \eta I(t), \tag{11}$$

where $N(t) = S(t) + I(t) + R(t)$. As $I(t) \geqslant 0$, we obtain

$${}_0^{ABC}D_t^{\alpha} N(t) \leqslant \Lambda - \mu N(t), \tag{12}$$

Consider the following initial value problem ${}_0^{ABC}D_t^{\alpha} N(t) = \Lambda - \mu N(t)$, with $N(0) = N_0$. Now applying Laplace transforms to both sides we obtain

$$L({}_0^{ABC}D_t^{\alpha} N(t) + \mu N(t)) = L(\Lambda). \tag{13}$$

Using equation (6), we obtain

$$\bar{N}(s) = \frac{\Lambda[(1-\alpha)s^{\alpha} + \alpha]}{s(\tau s^{\alpha} + \mu\alpha)} + \frac{s^{\alpha-1}N_0}{\tau s^{\alpha} + \mu\alpha}, \tag{14}$$

where $\tau = 1 + \mu(1-\alpha)$.

Further, equation (14) can be simplified as

$$\bar{N}(s) = \frac{\Lambda}{\mu}\left\{\frac{1}{s} - \frac{s^{\alpha-1}}{s^{\alpha} + \frac{\mu\alpha}{\tau}}\right\} + \frac{\Lambda(1-\alpha)}{\tau}\frac{s^{\alpha-1}}{s^{\alpha} + \frac{\mu\alpha}{\tau}} + \frac{N_0}{\tau}\frac{s^{\alpha-1}}{s^{\alpha} + \frac{\mu\alpha}{\tau}}. \tag{15}$$

Applying the inverse Laplace transform to (15) and using lemma 2 we obtain

$$N(t) = \frac{\Lambda}{\mu} + \left\{\frac{\Lambda(1-\alpha)\mu + \mu N_0 - \Lambda\tau}{\mu\tau}\right\} E_{\alpha}\left(-\frac{\mu\alpha}{\tau}t^{\alpha}\right). \tag{16}$$

It is observed that as $t \to +\infty$, and using the fact that ${}_0^{ABC}D_t^{\alpha} N(t) \leqslant \Lambda - \mu N(t), \ \alpha \in (0, 1]$, we have the following inequality $N(t) \leqslant \frac{\Lambda}{\mu}$. Thus, the solutions of model (8) are positively invariant and bounded in the region Ω.

Theorem 4. *The SIR model (8) has at most two equilibria namely (I) a disease-free equilibrium (DFE) E^0, and (II) an endemic equilibrium (EEP) E^*.*

Proof. In model (8), the susceptible and infected populations are independent of the recovered populations. Due to this fact, it is convenient to drop the third equation of the model (8). Hence model (8) can be recast as follows

$$\begin{aligned} {}^{ABC}_{0}D^{\alpha}_{t}S(t) &= \Lambda - \frac{\beta S(t)I(t)}{1+\xi_1 S(t)+\xi_2 I(t)} - \mu S(t), \\ {}^{ABC}_{0}D^{\alpha}_{t}I(t) &= \frac{\beta S(t)I(t)}{1+\xi_1 S(t)+\xi_2 I(t)} - \mu I(t) - \eta I(t) - \gamma I(t) - \frac{\varphi I(t)}{1+\rho I(t)}. \end{aligned} \tag{17}$$

Thus, to find the E^0 and E^* we solve the following equations

$$ {}^{ABC}_{0}D^{\alpha}_{t}S(t) = {}^{ABC}_{0} D^{\alpha}_{t}I(t) = 0. \tag{18}$$

Now combining equations (17) and (18) we have the following algebraic system

$$\begin{aligned} &\Lambda - \frac{\beta S(t)I(t)}{1+\xi_1 S(t)+\xi_2 I(t)} - \mu S(t) = 0, \\ &\frac{\beta S(t)I(t)}{1+\xi_1 S(t)+\xi_2 I(t)} - \mu I(t) - \eta I(t) - \gamma I(t) - \frac{\varphi I(t)}{1+\rho I(t)} = 0. \end{aligned} \tag{19}$$

By solving system (19), we obtain $E^0 = (S^0, I^0) = \left(\frac{\Lambda}{\mu}, 0\right)$, and $E^* = (S^*, I^*)$. Further information about E^* is provided in theorem 9.

5. Basic reproduction number

Here, we obtain the basic reproduction number (R_0) for the proposed model (8). In disease dynamics, R_0 captures the impact of model parameters on the spread of disease and so it plays a key role in developing any strategies for disease control. To find R_0 using a next-generation matrix method Diekmann *et al* (2010), we consider the following system

$$ {}^{ABC}_{0}D^{\alpha}_{t}x = F(x) - V(x), \tag{20}$$

where $x = [I, S]^T$.

The Jacobian matrices of new infected terms, $F(x)$, and other transfer terms, $V(x)$, at $E^0 = \left(\frac{\Lambda}{\mu}, 0\right)$ are given by

$$F(x) = \begin{pmatrix} \frac{\Lambda\beta}{\mu+\Lambda\xi_1} & 0 \\ 0 & 0 \end{pmatrix}, \quad V(x) = \begin{pmatrix} \varphi+\mu+\eta+\gamma & 0 \\ \frac{\Lambda\beta}{\mu+\Lambda\xi_1} & \mu \end{pmatrix}. \tag{21}$$

Now,

$$\begin{aligned} FV^{-1} &= \begin{pmatrix} \frac{\Lambda\beta}{\mu+\Lambda\xi_1} & 0 \\ 0 & 0 \end{pmatrix} \begin{pmatrix} \frac{1}{\varphi+\mu+\eta+\gamma} & 0 \\ -\frac{\Lambda\beta}{(\mu+\Lambda\xi_1)(\varphi+\mu+\eta+\gamma)\mu} & \frac{1}{\mu} \end{pmatrix}, \\ &= \begin{pmatrix} \frac{\Lambda\beta}{(\mu+\Lambda\xi_1)(\varphi+\mu+\eta+\gamma)} & 0 \\ 0 & 0 \end{pmatrix}. \end{aligned} \tag{22}$$

Therefore, R_0 is the spectral radius of the matrix FV^{-1} and is defined by the following expression

$$R_0 = \frac{\Lambda\beta}{(\mu+\Lambda\xi_1)(\varphi+\mu+\eta+\gamma)}. \tag{23}$$

Next, we derive the local stability analysis of the model (8) to determine whether the disease persists or not.

Theorem 5. *The disease-free equilibrium point $E^0 = (S^0, I^0) = \left(\frac{\Lambda}{\mu}, 0\right)$ of the model (8) is locally asymptotically stable if $R_0 < 1$. Otherwise, it is unstable.*

Proof. The Jacobian matrix of the model (8) is obtained as follows

$$J = \begin{pmatrix} J_{11} & J_{12} \\ J_{21} & J_{22} \end{pmatrix}, \tag{24}$$

where the components of J are given by

$$\begin{aligned} J_{11} &= -\mu - \frac{\beta I}{1+\xi_1 S+\xi_2 I} + \frac{\beta S I \xi_1}{(1+\xi_1 S+\xi_2 I)^2}, \\ J_{12} &= -\frac{\beta S}{1+\xi_1 S+\xi_2 I} + \frac{\beta S I \xi_2}{(1+\xi_1 S+\xi_2 I)^2}, \\ J_{21} &= \frac{\beta I}{1+\xi_1 S+\xi_2 I} - \frac{\beta S I \xi_1}{(1+\xi_1 S+\xi_2 I)^2}, \\ J_{22} &= \frac{\beta S}{1+\xi_1 S+\xi_2 I} - \frac{\beta S I \xi_2}{(1+\xi_1 S+\xi_2 I)^2} - (\mu+\eta+\gamma) - \frac{\varphi}{1+\rho I} + \frac{\varphi I \rho}{(1+\rho I)^2}. \end{aligned} \tag{25}$$

So the Jacobian matrix at E^0 is

$$J(E^0) = \begin{pmatrix} -\mu & -\frac{\Lambda\beta}{\mu+\Lambda\xi_1} \\ 0 & \frac{\Lambda\beta}{\mu+\Lambda\xi_1} - (\varphi+\mu+\eta+\gamma) \end{pmatrix}. \tag{26}$$

From equation (26) we see that the Jacobian matrix at E^0 is an upper triangular matrix. Hence the eigenvalues of $J(E^0)$ are

$$\begin{aligned} \lambda_1 &= -\mu, \\ \lambda_2 &= \frac{\Lambda\beta}{\mu+\Lambda\xi_1} - (\varphi+\mu+\eta+\gamma). \end{aligned} \tag{27}$$

The first eigenvalue is negative. To examine the nature of the second eigenvalue we rearrange it so that

$$\begin{aligned} \lambda_2 &= \frac{\Lambda\beta}{\mu+\Lambda\xi_1} - (\varphi+\mu+\eta+\gamma) \\ &= (\varphi+\mu+\eta+\gamma)\left\{\frac{\Lambda\beta}{(\mu+\Lambda\xi_1)(\varphi+\mu+\eta+\gamma)} - 1\right\} \\ &= (\varphi+\mu+\eta+\gamma)(R_0-1). \end{aligned} \tag{28}$$

It is now easily verified that $\lambda_2 < 0$ if $R_0 < 1$. Thus, the disease-free equilibrium of the model (8) is locally asymptotically stable if $R_0 < 1$, and it is otherwise unstable.

Theorem 6. *If $R_0 > 1$, then the model (8) possesses a unique endemic equilibrium point $E^* = (S^*, I^*)$.*

Proof. Let's consider the equation (19) at $E^* = (S^*, I^*)$ to explore the value of S^* and I^*.

$$\begin{aligned} &\Lambda - \frac{\beta S^* I^*}{1+\xi_1 S^*+\xi_2 I^*} - \mu S^* = 0, \\ &\frac{\beta S^* I^*}{1+\xi_1 S^*+\xi_2 I^*} - \mu I^* - \eta I^* - \gamma I^* - \frac{\varphi I^*}{1+\rho I^*} = 0. \end{aligned} \tag{29}$$

To find the value of S^* we rearranged the terms of the last equation of the system (29). Then the value of S^* in terms of I^* is

$$S^* = \frac{((\mu+\eta+\gamma)(1+\rho I^*)+\varphi)(1+\xi_2 I^*)}{\beta(1+\rho I^*) - \xi_1((\mu+\eta+\gamma)(1+\rho I^*)+\varphi)}. \tag{30}$$

Now from the first equation of system (29), we obtain the quadratic equation in S^* as

$$\mu\xi_1 S^{*2} + (\mu - \Lambda\xi_1 + (\mu\xi_2+\beta)I^*)S^* - \Lambda(1+\xi_2 I^*) = 0. \tag{31}$$

Substituting equation (30) in equation (31) gives the cubic equation in I^* as

$$c_0 + c_1 I^* + c_2 I^{*2} + c_3 I^{*3} = 0, \tag{32}$$

where

$$\begin{aligned}
c_0 &= \Lambda(\beta - \xi_1(\varphi + \mu + \eta + \gamma)) - \mu(\varphi + \mu + \eta + \gamma),\\
c_1 &= \Lambda\rho(2\beta - 2\xi_1(\mu + \eta + \gamma) - \xi_1\varphi) - \mu(\rho(\mu + \eta + \gamma) + (\varphi + \mu + \eta + \gamma)(\rho + \xi_2))\\
&\quad -(\varphi + \mu + \eta + \gamma)(\beta - \xi_1(\varphi + \mu + \eta + \gamma)),\\
c_2 &= \Lambda\rho^2(\beta - \xi_1(\mu + \eta + \gamma)) - \mu\rho(2\xi_2(\mu + \eta + \gamma) + \rho(\mu + \eta + \gamma) + \varphi\xi_2)\\
&\quad -(2\beta\rho(\mu + \eta + \gamma) - 2\rho\xi_1(\mu + \eta + \gamma)^2 - \rho\xi_1\varphi(\mu + \eta + \gamma)) - \varphi\rho(\beta - \xi_1(\mu + \eta + \gamma)),\\
c_3 &= -(\mu + \eta + \gamma)\rho^2(\mu\xi_2 + \beta - \xi_1(\mu + \eta + \gamma)).
\end{aligned} \tag{33}$$

Now the constant term c_0 can be modified as

$$\begin{aligned}
c_0 &= \Lambda(\beta - \xi_1(\varphi + \mu + \eta + \gamma)) - \mu(\varphi + \mu + \eta + \gamma)\\
&=\Lambda\beta - (\varphi + \mu + \eta + \gamma)(\mu + \Lambda\xi_1)\\
&=(\varphi + \mu + \eta + \gamma)(\mu + \Lambda\xi_1)(R_0 - 1).
\end{aligned} \tag{34}$$

It is easily seen that $c_0 > 0$ for $R_0 > 1$.

According to the fundamental theorem of algebra, the cubic equation (32) possesses at most three real non-negative roots. Here we focus on finding the endemic equilibrium. Using Descartes rule of signs Wang (2004), the equation (32) possesses a unique non-negative I^* under the following conditions:

$$\begin{aligned}
&(I)\, c_1 > 0,\ c_2 > 0,\ c_3 < 0;\\
&(II)\, c_1 > 0,\ c_2 < 0,\ c_3 < 0;\\
&(III)\, c_1 < 0,\ c_2 < 0,\ c_3 < 0.
\end{aligned} \tag{35}$$

If any of the conditions in (35) are satisfied, then there exists a unique non-negative I^*. Then, by using equation (30) we obtain the value of S^*. Hence the model (8) possesses a unique endemic equilibrium point $E^* = (S^*, I^*)$ if $R_0 > 1$.

Theorem 7. *The endemic equilibrium point $E^* = (S^*, I^*)$ of the model (8) is locally asymptotically stable if $R_0 > 1$ and under the following conditions*

$$\begin{aligned}
&(I)\, \frac{\beta S^*(1 + \xi_1 S^*)}{(1 + \xi_1 S^* + \xi_2 I^*)^2} < l_1,\\
&(II)\, \frac{\mu\beta S^*(1 + \xi_1 S^*)}{(1 + \xi_1 S^* + \xi_2 I^*)^2} < l_2,
\end{aligned} \tag{36}$$

where

$$\begin{aligned}
l_1 &= (2\mu + \eta + \gamma) + \frac{\varphi}{(1 + \rho I^*)^2} + \frac{\beta I^*(1 + \xi_2 I^*)}{(1 + \xi_1 S^* + \xi_2 I^*)^2},\\
l_2 &= \left(\mu + \frac{\beta I^*(1 + \xi_2 I^*)}{(1 + \xi_1 S^* + \xi_2 I^*)^2}\right)\left((\mu + \eta + \gamma) + \frac{\varphi}{(1 + \rho I^*)^2}\right).
\end{aligned} \tag{37}$$

Otherwise, it is unstable.

Proof. The Jacobian matrix of the model (8) is obtained as follows

$$J = \begin{pmatrix} J_{11} & J_{12} \\ J_{21} & J_{22} \end{pmatrix}, \tag{38}$$

where the components of J are defined in equation (25).

So the Jacobian matrix at E^* is

$$J(E^*) = \begin{pmatrix} -\mu - \frac{\beta I^*(1 + \xi_2 I^*)}{(1 + \xi_1 S^* + \xi_2 I^*)^2} & -\frac{\beta S^*(1 + \xi_1 S^*)}{(1 + \xi_1 S^* + \xi_2 I^*)^2} \\ \frac{\beta I^*(1 + \xi_2 I^*)}{(1 + \xi_1 S^* + \xi_2 I^*)^2} & \frac{\beta S^*(1 + \xi_1 S^*)}{(1 + \xi_1 S^* + \xi_2 I^*)^2} - (\mu + \eta + \gamma) - \frac{\varphi}{(1 + \rho I^*)^2} \end{pmatrix}. \tag{39}$$

The characteristic equation of the Jacobian matrix at the endemic equilibrium point $J(E^*)$ is $\det(J(E^*) - \lambda I) = 0$.

Thus, we have

$$\lambda^2 + a_1\lambda + a_2 = 0, \tag{40}$$

where

$$a_1 = (2\mu + \eta + \gamma) + \frac{\beta I^*(1+\xi_2 I^*)}{(1+\xi_1 S^* + \xi_2 I^*)^2} - \frac{\beta S^*(1+\xi_1 S^*)}{(1+\xi_1 S^* + \xi_2 I^*)^2} + \frac{\varphi}{(1+\rho I^*)^2},$$
$$a_2 = \left(\mu + \frac{\beta I^*(1+\xi_2 I^*)}{(1+\xi_1 S^* + \xi_2 I^*)^2}\right)\left((\mu + \eta + \gamma) + \frac{\varphi}{(1+\rho I^*)^2}\right) - \frac{\mu\beta S^*(1+\xi_1 S^*)}{(1+\xi_1 S^* + \xi_2 I^*)^2}, \tag{41}$$

Then the Routh-Hurwitz stability criteria Matignon (1996) confirm that the roots of equation (40) have negative real parts provided that $a_i > 0,\ i = 1, 2$.

Thus, the endemic equilibrium point $E^* = (S^*, I^*)$ of the model (8) is locally asymptotically stable if equation (36) holds.

Lemma 8. *Taneco-Hernández and Vargas-De-León (2020) Let $f(t) \in R^+$ be a differentiable and continuous function. Then for any $f^* \in R^+$ and $\alpha \in (0, 1)$, we have*

$${}_0^{ABC}D_t^{\alpha}\left[f(t) - f^* - f^* \ln\frac{f(t)}{f^*}\right] \leqslant \left(1 - \frac{f^*}{f(t)}\right){}_0^{ABC}D_t^{\alpha} f(t). \tag{42}$$

Theorem 9. *The disease-free equilibrium point $E^0 = (S^0, I^0) = \left(\frac{\Lambda}{\mu}, 0\right)$ of the model (8) is globally asymptotically stable if $R_0 \leqslant 1$ and $\varphi = 0$. For $\varphi \neq 0$, E^0 is globally asymptotically stable if $R_1 \leqslant 1$.*

Proof. Consider a candidate positive definite Lyapunov function $L(S, I)$: $\Omega \to R^+$ defined by

$$L(t) = \frac{1}{1+\xi_1 S^0}\left(S(t) - S^0 - S^0 \ln\frac{S(t)}{S^0}\right) + I(t). \tag{43}$$

Applying the ABC derivative on both the side of equation (43), we have

$${}_0^{ABC}D_t^{\alpha} L(t) = {}_0^{ABC}D_t^{\alpha}\left\{\frac{1}{1+\xi_1 S^0}\left(S(t) - S^0 - S^0 \ln\frac{S(t)}{S^0}\right) + I(t)\right\}. \tag{44}$$

Then by using the linearity property and lemma 8 on equation (44), we have

$${}_0^{ABC}D_t^{\alpha} L(t) \leqslant \frac{1}{1+\xi_1 S^0}\left(1 - \frac{S^0}{S}\right){}_0^{ABC}D_t^{\alpha} S(t) + {}_0^{ABC}D_t^{\alpha} I(t). \tag{45}$$

From (8) we get

$${}_0^{ABC}D_t^{\alpha} L(t) \leqslant \frac{1}{1+\xi_1 S^0}\left(1 - \frac{S^0}{S}\right)\left(\Lambda - \frac{\beta S(t) I(t)}{1+\xi_1 S(t) + \xi_2 I(t)} - \mu S(t)\right)$$
$$+\left(\frac{\beta S(t) I(t)}{1+\xi_1 S(t) + \xi_2 I(t)} - \mu I(t) - \eta I(t) - \gamma I(t) - \frac{\varphi I(t)}{1+\rho I(t)}\right). \tag{46}$$

Since $S^0 = \frac{\Lambda}{\mu}$, it follows that

$${}_0^{ABC}D_t^{\alpha} L(t) \leqslant \frac{1}{1+\xi_1 S^0}\left(\mu S^0 - \frac{\beta S(t) I(t)}{1+\xi_1 S(t) + \xi_2 I(t)} - \mu S(t)\right)$$
$$-\frac{1}{1+\xi_1 S^0}\frac{S^0}{S}\left(\mu S^0 - \frac{\beta S(t) I(t)}{1+\xi_1 S(t) + \xi_2 I(t)} - \mu S(t)\right)$$
$$+\left(\frac{\beta S(t) I(t)}{1+\xi_1 S(t) + \xi_2 I(t)} - (\mu + \eta + \gamma) I(t) - \frac{\varphi I(t)}{1+\rho I(t)}\right). \tag{47}$$

Then using $R_0 = \frac{\Lambda\beta}{(\mu + \Lambda\xi_1)(\varphi + \mu + \eta + \gamma)}$, and simple rearrangements, lead us to

$${}_0^{ABC}D_t^{\alpha} L(t) \leqslant -\frac{\mu(S(t) - S^0)^2}{S(t)(1+\xi_1 S^0)} - \frac{(\mu + \eta + \gamma)\xi_2}{1+\xi_1 S(t) + \xi_2 I(t)} I^2(t) - \frac{\varphi I(t)}{1+\rho I(t)}$$
$$+\frac{\xi_1 S(t) I(t)}{1+\xi_1 S(t) + \xi_2 I(t)}\left\{(\varphi + \mu + \eta + \gamma) R_0 - (\mu + \eta + \gamma) + \frac{\varphi}{\xi_1 S(t)}\right\}$$
$$+\frac{(\varphi + \mu + \eta + \gamma) I(t)}{1+\xi_1 S(t) + \xi_2 I(t)}(R_0 - 1). \tag{48}$$

Next, we discuss two cases based on φ.

Case I: $\varphi = 0$

If $\varphi = 0$, then equation (48) is reduced to

$$
\begin{aligned}
{}_{0}^{ABC}D_{t}^{\alpha}L(t) \leqslant & -\frac{\mu(S(t)-S^{0})^{2}}{S(t)(1+\xi_{1}S^{0})} - \frac{(\mu+\eta+\gamma)\xi_{2}}{1+\xi_{1}S(t)+\xi_{2}I(t)}I^{2}(t) \\
& + \frac{(\mu+\eta+\gamma)I(t)(1+\xi_{1}S(t))}{1+\xi_{1}S(t)+\xi_{2}I(t)}(R_{0}-1).
\end{aligned} \tag{49}
$$

Thus ${}_{0}^{ABC}D_{t}^{\alpha}L(t) < 0$ if $R_0 \leqslant 1$ and ${}_{0}^{ABC}D_{t}^{\alpha}L(t) = 0$ if $S(t) = S^0$ and $I(t) = I^0 = 0$.

Case II: $\varphi \neq 0$

If $\varphi \neq 0$, then equation (48) is reduced to

$$
\begin{aligned}
{}_{0}^{ABC}D_{t}^{\alpha}L(t) \leqslant & -\frac{\mu(S(t)-S^{0})^{2}}{S(t)(1+\xi_{1}S^{0})} - \frac{(\mu+\eta+\gamma)\xi_{2}}{1+\xi_{1}S(t)+\xi_{2}I(t)}I^{2}(t) - \frac{\varphi I(t)}{1+\rho I(t)} \\
& + \frac{\xi_{1}S(t)I(t)}{1+\xi_{1}S(t)+\xi_{2}I(t)}P + \frac{(\varphi+\mu+\eta+\gamma)I(t)}{1+\xi_{1}S(t)+\xi_{2}I(t)}(R_{0}-1),
\end{aligned} \tag{50}
$$

where $P = (\varphi+\mu+\eta+\gamma)R_0 - (\mu+\eta+\gamma) + \frac{\varphi}{\xi_1 S(t)}$.

Thus ${}_{0}^{ABC}D_{t}^{\alpha}L(t) < 0$ if $P < 0$. This means that $(\varphi+\mu+\eta+\gamma)R_0 + \frac{\varphi}{\xi_1 S(t)} \leqslant (\mu+\eta+\gamma)$ and $R_0 \leqslant 1$.

Further modification gives $R_1 = \frac{(\varphi+\mu+\eta+\gamma)R_0 + \frac{\varphi}{\xi_1 S(t)}}{(\mu+\eta+\gamma)} \leqslant 1$. Also, it is clear that ${}_{0}^{ABC}D_{t}^{\alpha}L(t) = 0$ if $S(t) = S^0$ and $I(t) = I^0 = 0$.

Theorem 10. *The endemic equilibrium point $E^* = (S^*, I^*)$ of the model (8) is globally asymptotically stable if $R_0 > 1$ and under the following condition:*

$$
\frac{\beta^{2}\xi_{2}S^{*}I^{*}(1+\xi_{2}I^{*})}{(1+\xi_{1}S^{*}+\xi_{2}I^{*})^{2}} < m_{1}m_{2}, \tag{51}
$$

where

$$
\begin{aligned}
m_{1} &= \mu + \frac{\mu\beta I^{*}(1+\xi_{2}I^{*})}{(\mu+\Lambda(\xi_{1}+\xi_{2}))(1+\xi_{1}S^{*}+\xi_{2}I^{*})}, \\
m_{2} &= \frac{\mu\beta\xi_{2}S^{*}}{(\mu+\Lambda(\xi_{1}+\xi_{2}))(1+\xi_{1}S^{*}+\xi_{2}I^{*})}.
\end{aligned} \tag{52}
$$

Otherwise, it is unstable.

Proof. Consider a candidate positive definite Lyapunov function $L(S, I)$: $\Omega \to R^+$ defined by

$$
L(t) = \frac{1}{2}(S(t)-S^{*})^{2} + \left(I(t) - I^{*} - I^{*}\ln\frac{I(t)}{I^{*}}\right). \tag{53}
$$

Applying the ABC derivative to both the side of equation (53), we have

$$
{}_{0}^{ABC}D_{t}^{\alpha}L(t) = {}_{0}^{ABC}D_{t}^{\alpha}\left\{\frac{1}{2}(S(t)-S^{*})^{2} + \left(I(t) - I^{*} - I^{*}\ln\frac{I(t)}{I^{*}}\right)\right\}. \tag{54}
$$

Then by using the linearity property and lemma 8 on equation (54), we have

$$
{}_{0}^{ABC}D_{t}^{\alpha}L(t) \leqslant (S(t)-S^{*})\,{}_{0}^{ABC}D_{t}^{\alpha}S(t) + \left(1-\frac{I^{*}}{I}\right){}_{0}^{ABC}D_{t}^{\alpha}I(t). \tag{55}
$$

Substituting the values of ${}_{0}^{ABC}D_{t}^{\alpha}S(t)$ and ${}_{0}^{ABC}D_{t}^{\alpha}I(t)$ into equation (55), and simple rearrangement, gives the following expression

$$
{}_{0}^{ABC}D_{t}^{\alpha}L(t) \leqslant -a_{1}(S(t)-S^{*})^{2} + a_{2}(S(t)-S^{*})(I(t)-I^{*}) - a_{3}(I(t)-I^{*}), \tag{56}
$$

Table 2. Parameters and their numerical values Swati (2022).

Parameter	Λ	μ	β	ξ_1	ξ_2	η	γ	φ	ρ
Numerical value	5	0.05	0.003	0.003	0.002	0.05	0.003	0.03	0.002

Table 3. Random set of initial conditions.

Initial condition (IC)	IC1	IC2	IC3	IC4	IC5	IC6	IC7
S_0	20	30	11	15	60	70	80
I_0	3	8	27	35	40	30	20

where

$$a_1 = \mu + \frac{\beta I^*(1+\xi_2 I^*)}{(1+\xi_1 S+\xi_2 I)(1+\xi_1 S^*+\xi_2 I^*)},$$
$$a_2 = \frac{\beta\xi_2 S^* I^*}{(1+\xi_1 S+\xi_2 I)(1+\xi_1 S^*+\xi_2 I^*)} - \frac{\beta S}{(1+\xi_1 S+\xi_2 I)} + \frac{\beta(1+\xi_2 I^*)}{(1+\xi_1 S+\xi_2 I)(1+\xi_1 S^*+\xi_2 I^*)},$$
$$a_3 = \frac{\beta\xi_2 S^*}{(1+\xi_1 S+\xi_2 I)(1+\xi_1 S^*+\xi_2 I^*)} - \frac{\varphi\rho}{(1+\rho I)(1+\rho I^*)}. \tag{57}$$

Thus ${}_0^{ABC}D_t^{\alpha} L(t) < 0$ if $a_1 > 0$ and $a_2^2 < 4a_1 a_2$.

It is clear that $a_1 > 0$ for all $E^* = (S^*, I^*)$. Also, the condition $a_2^2 < 4a_1 a_2$ is satisfied if $\frac{\beta^2\xi_2 S^* I^*(1+\xi_2 I^*)}{(1+\xi_1 S^*+\xi_2 I^*)^2} < m_1 m_2$.

Thus, the endemic equilibrium point $E^* = (S^*, I^*)$ of the model (8) is globally asymptotically stable if equation (51) holds.

6. Numerical results

In this section, we perform a numerical simulation of the model (8) to validate the analytical work. The numerical values of the biological parameters used in the simulation are defined in table 2.

For the given set of values, we calculated the endemic equilibrium point of the model (8) as $E^* = (S^*, I^*) = (52.6, 17.97)$. This value satisfies the result of theorem 10. Next, to show that E^* is globally asymptotically stable, we consider a random set of initial conditions as defined in table 3.

Figure 1 is simulated for seven random sets of initial conditions for the susceptible and infected population. All solution trajectories corresponding to various different initial conditions approach the equilibrium $E^* = (52.6, 17.97)$ asymptotically, irrespective of the starting point. Thus from this numerical result, it is observed that E^* is globally asymptotically stable.

The initial conditions used in the numerical simulation are chosen as $S_0 = 94$, $I_0 = 6$, and $R_0 = 0$ for susceptible, infected, and recovered populations, respectively. Using the numerical scheme developed by M. Toufik and A. Atangana Toufik and Atangana (2017), model (8) is simulated to observe the effects of face mask, social distancing, quarantine, lockdown, immigration, treatment rate of disease, limitation in treatment resources, and also different orders of ABC derivative. The order of the ABC derivative is chosen as $\alpha = 0.8,\ 0.9,\ 1$ in figures 2(a) to (c), respectively.

Figure 2 shows the transmission dynamics of the state variables with an arbitrarily chosen time interval of 300 days. It is observed from figure 2(a), that as time increases the susceptible population is decreased and as a consequence, the infected population is increasing. Finally, the susceptible and infected populations move to achieve a steady state equilibrium E^*. A sharp fall and pick up is observed in the susceptible, infected, and recovered population in the case of the ABC derivative with $\alpha = 1$. As the fractional order decreases, the sharp fall and pick up gradually vanish due to the non-local and non-singular effects of the ABC derivative and faster attainment of the equilibrium steady state.

Figure 3 illustrates the effect of preventive measures taken by susceptible populations, such as the proper use of face masks and social distancing, on the transmission dynamics of the infected population. It is observed from figure 3(a)–(c), that if the use of face masks and social distancing is properly followed, so that the value of ξ_1 is

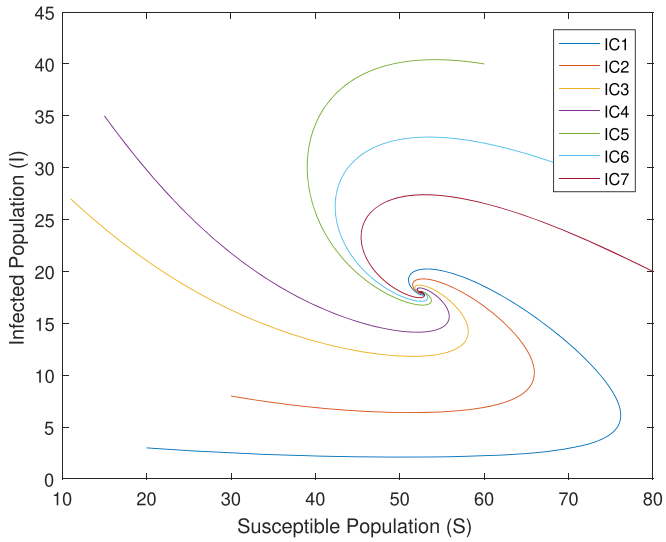

Figure 1. Global stability of endemic equilibrium point.

increased, then the infected population dramatically decreases, and moves towards an equilibrium state. The profile suddenly attains a pick-up for the first 50 days and then decreases but the pick-up gradually vanishes due to the ABC derivative as it includes the memory of infected populations.

Figure 4 illustrates the effect of preventive measures taken by the infected population, such as quarantine and self-isolation, on the transmission dynamics of the infected population. It is observed from figures 4(a)–(c) that if the quarantine and self-isolation for infective populations are properly followed, so that the value of ξ_2 is increased, then the infected population dramatically decreases. The decrease in the infected population means a corresponding increase in the susceptible or recovered populations.

The common population-wide effort to reduce transmission of COVID-19 is to impose a lockdown. Figures 5(a)–(c) show the effect of lockdown on the infected population for ABC derivatives $\alpha = 0.8, 0.9, 1$ respectively. It is observed from figures 5(a)–(c), that as the lockdown is imposed, then the disease transmission rate is decreased, and ultimately the infected population is decreased. Also, from figure 5 it is observed that the lockdown and memory effect plays a vital role in reducing the infected populations.

Sealing borders, closing entry into a country, or restricting air, sea, and other forms of travel, are common measures used to reduce infection rates. Figure 6 shows the effect of travel (i.e. immigration) on the infected population over time t. It is observed from figures 6(a)–(c) that as immigration is restricted, there is a dramatic reduction in the infected populations. As the value of Λ is increased, so there is a sudden rise in the infected population due to the new arrival of an infected immigrant population.

Figure 7 shows the effect of treatment rates on the transmission dynamics of the infected population. It is observed from figures 7(a)–(c), that with an increase in treatment rates such as better access to hospital facilities, vaccination, awareness, and cure, that is with an increasing value of φ, then there are dramatic falls in the infected population number. Also, it is observed that in figure 7(c) the infected population rises suddenly and attains a sharp pick as compared to figure 7(a). It can be interpreted that this situation arises from the ABC derivative. Due to the ABC derivative or memory of the infected population, a gradual reduction in the initial days and a sharp pick is observed.

Figure 8 shows the effect of a limitation in treatment availability on the infected population. It is observed from figures 8(a)–(c), that with a limitation in a hospital facility, lack of a vaccine or lack of oxygen cylinder, and so an increase in ρ, then the infected population increases.

7. Conclusion

In this paper, we developed an SIR model with the ABC derivative to investigate the effects of face masks, social distancing, quarantine, lockdown, immigration, treatment rate of disease, and limitation in treatment resources. A Beddington-DeAngelis infection rate and Holling type-II treatment rate were used to capture the impact of model parameters on the infected population. The SIR model (8) with the ABC derivative has possessed two equilibrium points, namely disease-free and endemic equilibrium points. The disease-free equilibrium point of the model (8) is locally asymptotically stable if $R_0 < 1$. The endemic equilibrium point of the model (8) is locally asymptotically stable if $R_0 > 1$ and under the conditions given in inequality (36). The disease-free equilibrium

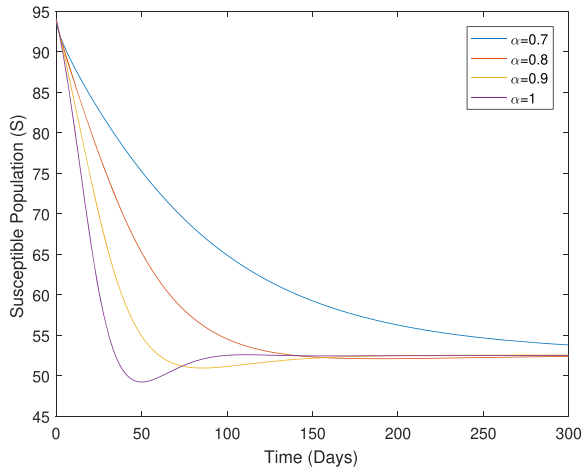

(a)

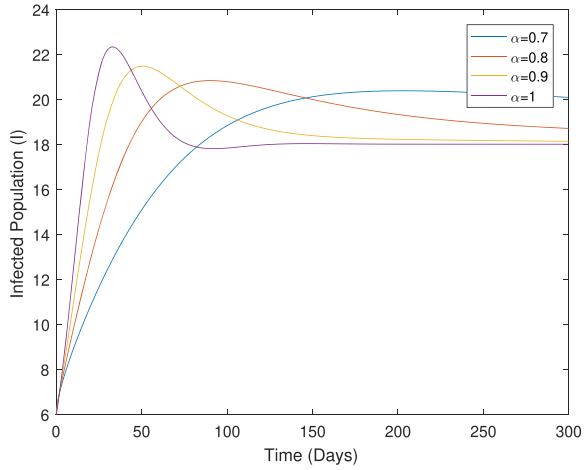

(b)

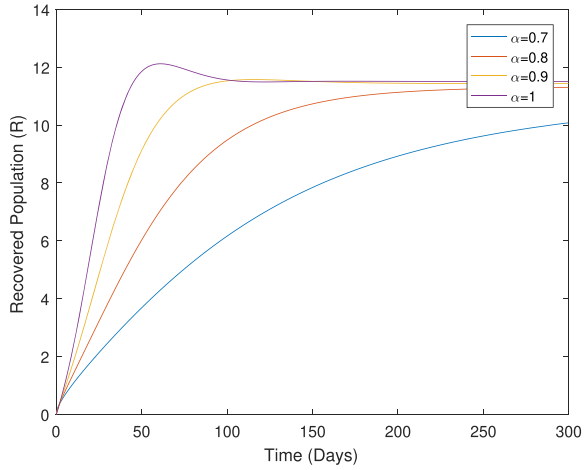

(c)

Figure 2. (a) Dynamical behavior for the susceptible population for different ABC derivative orders (b) Dynamical behavior for the infected population for different ABC derivative orders (c) Dynamical behavior for the recovered population for different ABC derivative orders.

point of the model (8) is globally asymptotically stable if $R_0 \leqslant 1$ and $\varphi = 0$. When $\varphi \neq 0$, the model is globally asymptotically stable if $R_1 \leqslant 1$. The endemic equilibrium point of the model (8) is globally asymptotically stable if $R_0 > 1$ and under the conditions of inequality (51). The global stability of the endemic equilibrium point has been also shown by the numerical results. From the numerical results, it has been observed that face masks and

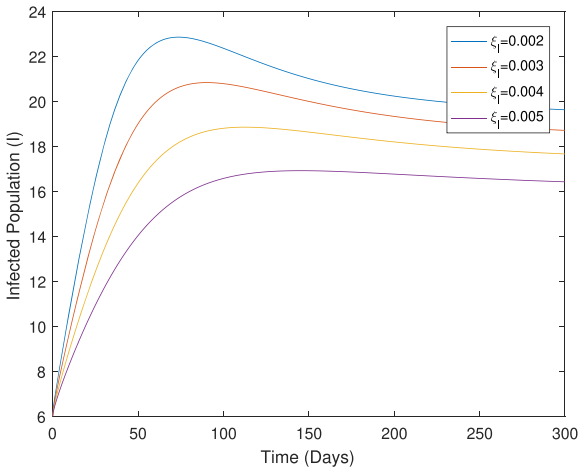

(a)

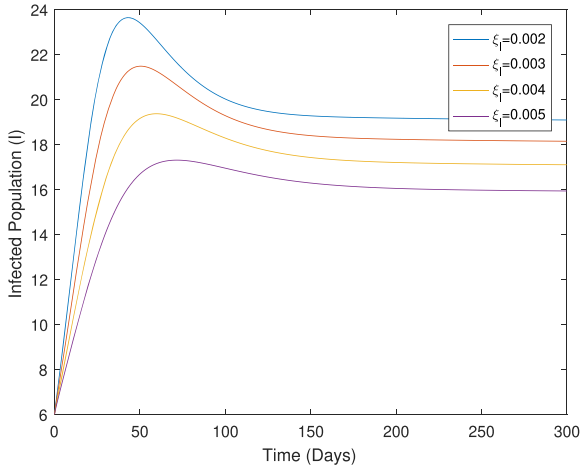

(b)

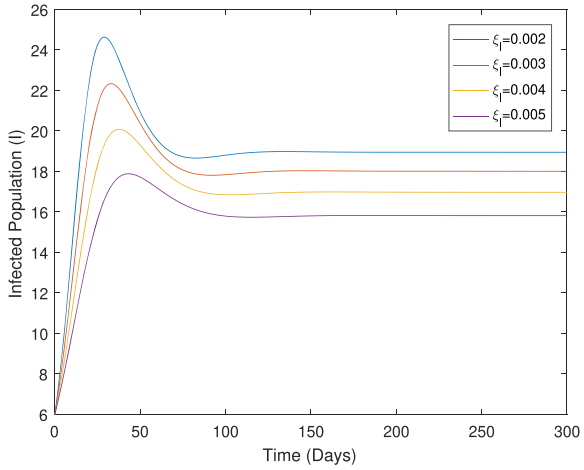

(c)

Figure 3. Effect of face mask and social distance on infected population for (a) $\alpha = 0.8$ (b) $\alpha = 0.9$ (c) $\alpha = 1$.

social distancing reduce the infected population. Also, quarantine, lockdown, restricted immigration, and effective treatment rates significantly reduce the infected population over time, whereas limitation in the availability of treatment raises the infected population. Furthermore, the numerical results suggest that COVID-19 can be reduced or eliminated from the community by adhering to the guideline of WHO such as the proper

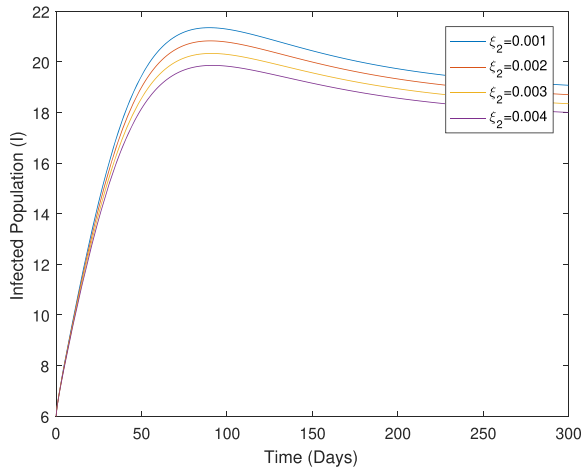

(a)

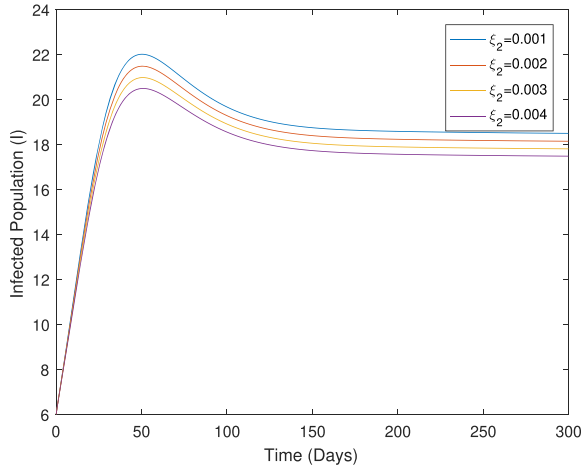

(b)

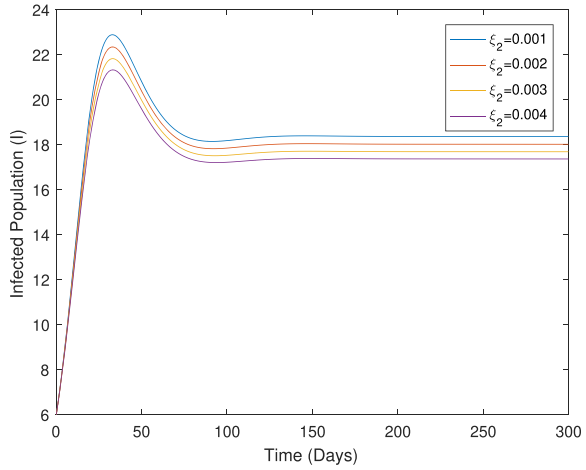

(c)

Figure 4. Effect of quarantine on infected population for (a) $\alpha = 0.8$ (b) $\alpha = 0.9$ (c) $\alpha = 1$.

wearing of face masks, social distancing, quarantine, lockdown, and restricted immigration. The non-local and non-singular properties of the ABC derivative have advantages compared with integer-order derivative models in which we require more compartments to capture the disease complexity. The present model can be further used to develop a control strategy or predict the number of the infected population in future pandemics.

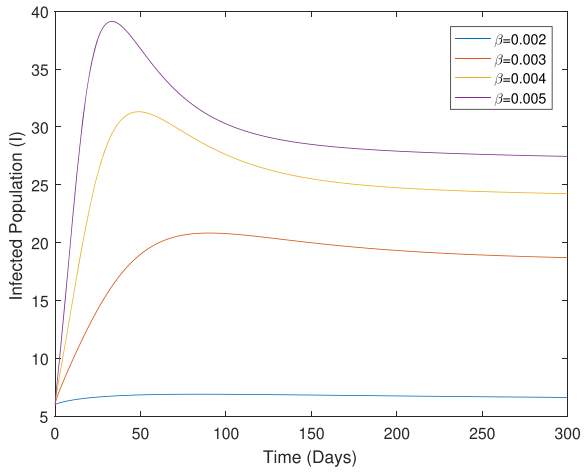

(a)

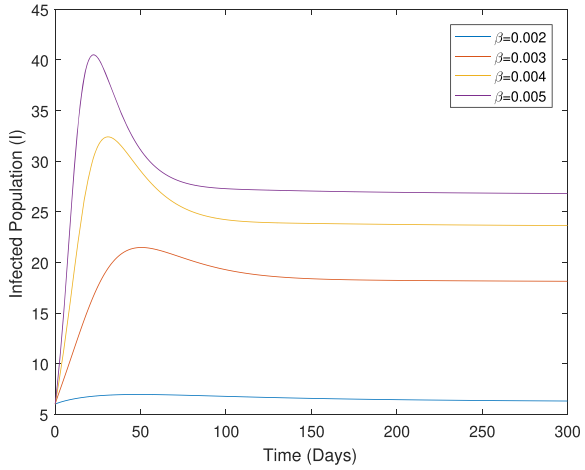

(b)

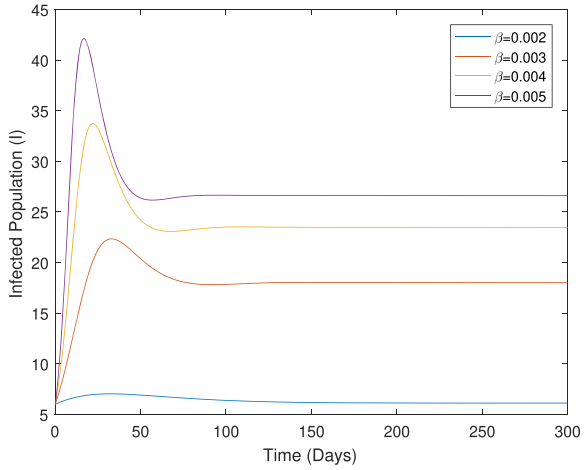

(c)

Figure 5. Effect of lockdown on infected population for (a) $\alpha = 0.8$ (b) $\alpha = 0.9$ (c) $\alpha = 1$.

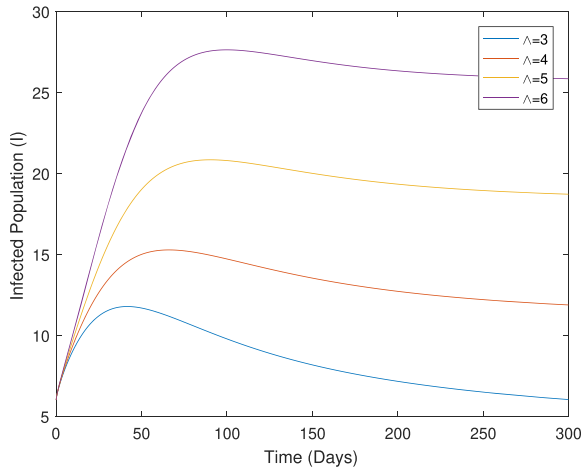

(a)

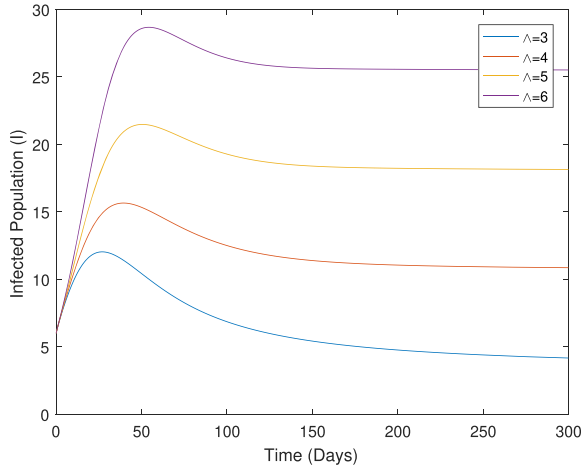

(b)

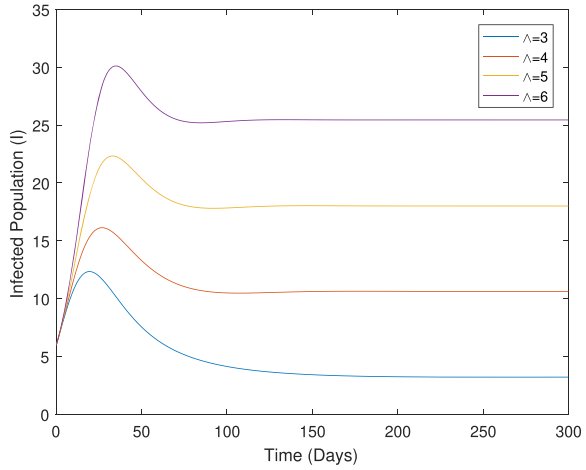

(c)

Figure 6. Effect of immigration on infected population for (a) $\alpha = 0.8$ (b) $\alpha = 0.9$ (c) $\alpha = 1$.

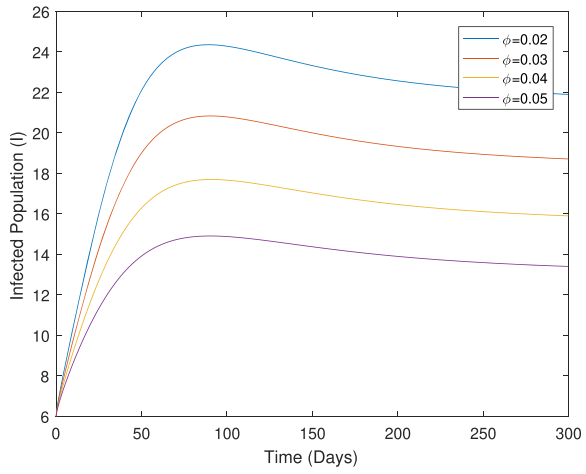

(a)

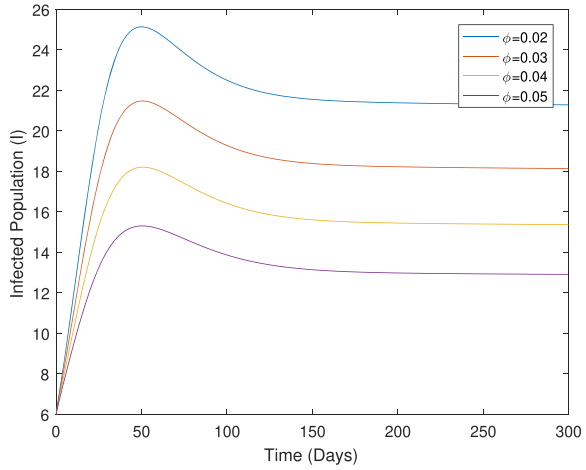

(b)

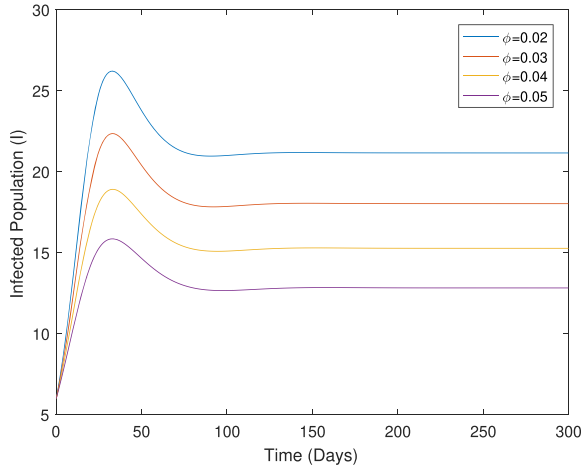

(c)

Figure 7. Effect of treatment rate of disease on infected population for (a) $\alpha = 0.8$ (b) $\alpha = 0.9$ (c) $\alpha = 1$.

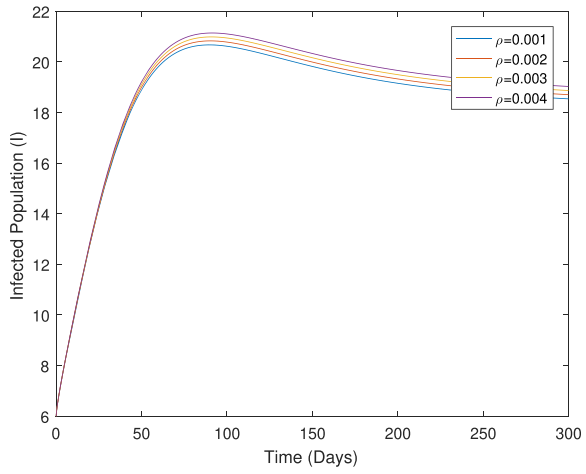

(a)

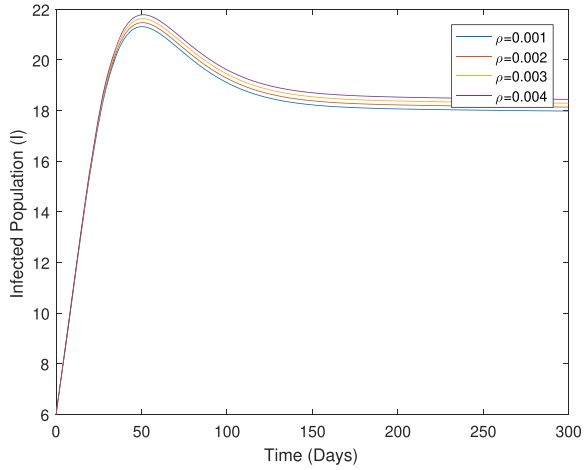

(b)

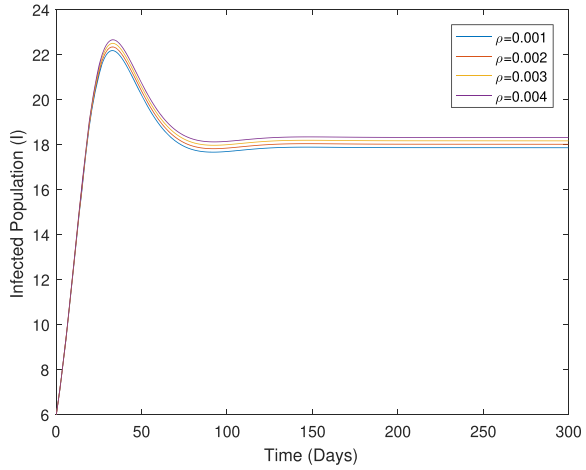

(c)

Figure 8. Effect of limitation in treatment availability on infected population for (a) $\alpha = 0.8$ (b) $\alpha = 0.9$ (c) $\alpha = 1$.

Acknowledgments

The authors would like to thank the reviewers and editors of this paper for their careful attention to detail and constructive feedback that improved the presentation of the paper greatly. M. Yavuz was supported by TUBITAK (The Scientific and Technological Research Council of Türkiye).

Data availability statement

No new data were created or analysed in this study.

Competing interests

The authors have no competing interests to declare.

ORCID iDs

Mehmet Yavuz https://orcid.org/0000-0002-3966-6518

References

Ahmad S, Qiu D and ur Rahman M 2022 Dynamics of a fractional-order COVID-19 model under the nonsingular kernel of Caputo-Fabrizio operator *Mathematical Modelling and Numerical Simulation with Applications* **2** 228–43

Allegretti S, Bulai I M, Marino R, Menandro M A and Parisi K 2021 Vaccination effect conjoint to fraction of avoided contacts for a sars-cov-2 mathematical model *Mathematical Modelling and Numerical Simulation with Applications* **1** 56–66

Atangana A 2020 Modelling the spread of covid-19 with new fractal-fractional operators: can the lockdown save mankind before vaccination? *Chaos, Solitons Fractals* **136** 109860

Atangana A and Baleanu D 2016 New fractional derivatives with nonlocal and non-singular kernel: theory and application to heat transfer model *Thermal Science* **20** 763–9

Baleanu D, Diethelm K, Scalas E and Trujillo J J 2012 *Fractional Calculus: Models and Numerical Methods* vol. 3 (Singapore: World Scientific)

Beddington J R 1975 Mutual interference between parasites or predators and its effect on searching efficiency *The Journal of Animal Ecology* **44** 331–40

Biswas S K, Ghosh J K, Sarkar S and Ghosh U 2020 Covid-19 pandemic in India: a mathematical model study *Nonlinear Dyn.* **102** 537–53

DeAngelis D L, Goldstein R A and O'Neill R V 1975 A model for tropic interaction *Ecology* **56** 881–92

Diekmann O, Heesterbeek J and Roberts M G 2010 The construction of next-generation matrices for compartmental epidemic models *Journal of the Royal Society Interface* **7** 873–85

Erturk V S and Kumar P 2020 Solution of a covid-19 model via new generalized Caputo-type fractional derivatives *Chaos, Solitons Fractals* **139** 110280

Gao W, Veeresha P, Baskonus H M, Prakasha D G and Kumar P 2020 A new study of unreported cases of 2019-ncov epidemic outbreaks *Chaos, Solitons Fractals* **138** 109929

Guo Y and Li T 2022 Modeling and dynamic analysis of novel coronavirus pneumonia (covid-19) in china *J. Appl. Math. Comput.* **68** 2641–66

Hanert E, Schumacher E and Deleersnijder E 2011 Front dynamics in fractional-order epidemic models *J. Theor. Biol.* **279** 9–16

Haq I U, Ali N and Nisar K S 2022 An optimal control strategy and grünwald-letnikov finite-difference numerical scheme for the fractional-order covid-19 model *Mathematical Modelling and Numerical Simulation with Applications* **2** 108–16

Joshi H and Jha B K 2018 Fractional reaction diffusion model for parkinson's disease *International Conference on ISMAC in Computational Vision and Bio-Engineering, Springer* 1739–48

Joshi H and Jha B K 2021a Chaos of calcium diffusion in parkinson's infectious disease model and treatment mechanism via hilfer fractional derivative *Mathematical Modelling and Numerical Simulation with Applications* **1** 84–94

Joshi H and Jha B K 2021b Modeling the spatiotemporal intracellular calcium dynamics in nerve cell with strong memory effects *International Journal of Nonlinear Sciences and Numerical Simulation* (https://doi.org/10.1515/ijnsns-2020-0254)

Joshi H and Jha B K 2022 Generalized diffusion characteristics of calcium model with concentration and memory of cells: a spatiotemporal approach *Iranian Journal of Science and Technology, Transactions A: Science* **46** 309–22

Joshi H, Jha B K and Yavuz M 2023 Modelling and analysis of fractional-order vaccination model for control of covid-19 outbreak using real data *Mathematical Biosciences and Engineering* **20** 213–40

Karim F, Chauhan S and Dhar J 2022 Analysing an epidemic-economic model in the presence of novel corona virus infection: capital stabilization, media effect, and the role of vaccine *The European Physical Journal Special Topics* **231** 1–18

Kumar P and Erturk V S 2021 Dynamics of cholera disease by using two recent fractional numerical methods *Mathematical Modelling and Numerical Simulation with Applications* **1** 102–11

Kumar S, Chauhan R P, Momani S and Hadid S 2020 Numerical investigations on covid-19 model through singular and non-singular fractional operators *Numerical Methods for Partial Differential Equations* (https://doi.org/10.1002/num.22707)

Kurmi S and Chouhan U 2022 A multicompartment mathematical model to study the dynamic behaviour of covid-19 using vaccination as control parameter *Nonlinear Dyn.* **109** 2185–201

Li T and Guo Y 2022 Modeling and optimal control of mutated covid-19 (delta strain) with imperfect vaccination *Chaos, Solitons Fractals* **156** 111825

Li T and Guo Y 2022 Optimal control and cost-effectiveness analysis of a new covid-19 model for omicron strain *Physica A* **606** 128134

Ma Z, Wang S, Lin X, Li X, Han X, Wang H and Liu H 2022 Modeling for covid-19 with the contacting distance *Nonlinear Dyn.* **107** 3065–84

Magin R 2004 Fractional calculus in bioengineering, part 1 *Critical Reviews™ in Biomedical Engineering* **32** 1–104

Matignon D 1996 Stability results for fractional differential equations with applications to control processing *Computational Engineering in Systems Applications* **2** 963–8
Memon Z, Qureshi S and Memon B R 2021 Assessing the role of quarantine and isolation as control strategies for covid-19 outbreak: a case study *Chaos, Solitons Fractals* **144** 110655
Mishra A M, Purohit S D, Owolabi K M and Sharma Y D 2020 A nonlinear epidemiological model considering asymptotic and quarantine classes for sars cov-2 virus *Chaos, Solitons Fractals* **138** 109953
Nabi K N, Kumar P and Erturk V S 2021 Projections and fractional dynamics of covid-19 with optimal control strategies *Chaos, Solitons Fractals* **145** 110689
Naik P A, Owolabi K M, Zu J and Naik M-U-D 2021 Modeling the transmission dynamics of covid-19 pandemic in caputo type fractional derivative *Journal of Multiscale Modelling* **12** 2150006
Naik P A, Yavuz M, Qureshi S, Zu J and Townley S 2020a Modeling and analysis of covid-19 epidemics with treatment in fractional derivatives using real data from pakistan *The European Physical Journal Plus* **135** 1–42
Naik P A, Yavuz M and Zu J 2020b The role of prostitution on hiv transmission with memory: a modeling approach *Alexandria Engineering Journal* **59** 2513–31
Özköse F and Yavuz M 2022 Investigation of interactions between covid-19 and diabetes with hereditary traits using real data: a case study in turkey *Comput. Biol. Med.* **141** 105044
Özköse F, Yavuz M, Şenel M T and Habbireeh R 2022 Fractional order modelling of omicron sars-cov-2 variant containing heart attack effect using real data from the united kingdom *Chaos, Solitons Fractals* **157** 111954
Pandey P, Gómez-Aguilar J F, Kaabar M K, Siri Z and Abd Allah A M 2022 Mathematical modeling of covid-19 pandemic in india using caputo-fabrizio fractional derivative *Comput. Biol. Med.* **145** 105518
Pérez A G and Oluyori D A 2022 A model for covid-19 and bacterial pneumonia coinfection with community-and hospital-acquired infections *Mathematical Modelling and Numerical Simulation with Applications* **2** 197–210
Podlubny I 1998 *Fractional Differential Equations: An Introduction to Fractional Derivatives, Fractional Differential Equations, to Methods of Their Solution and Some of Their Applications* (Amsterdam: Elsevier)
Rajagopal K, Hasanzadeh N, Parastesh F, Hamarash I I, Jafari S and Hussain I 2020 A fractional-order model for the novel coronavirus (covid-19) outbreak *Nonlinear Dyn.* **101** 711–8
Safare K M, Betageri V S, Prakasha D G, Veeresha P and Kumar S 2021 A mathematical analysis of ongoing outbreak covid-19 in india through nonsingular derivative *Numerical Methods for Partial Differential Equations* **37** 1282–98
Sene N 2020 Analysis of the stochastic model for predicting the novel coronavirus disease *Advances in Difference Equations* **2020** 1–19
Sitthiwirattham T, Zeb A, Chasreechai S, Eskandari Z, Tilioua M and Djilali S 2021 Analysis of a discrete mathematical covid-19 model *Results in Physics* **28** 104668
Srivastav A K, Tiwari P K, Srivastava P K, Ghosh M and Kang Y 2021 A mathematical model for the impacts of face mask, hospitalization and quarantine on the dynamics of covid-19 in India: deterministic versus stochastic *Mathematical Biosciences and Engineering* **18** 182–213
Sun G-Q, Wang S-F, Li M-T, Li L, Zhang J, Zhang W, Jin Z and Feng G-L 2020 Transmission dynamics of covid-19 in Wuhan, China: effects of lockdown and medical resources *Nonlinear Dyn.* **101** 1981–93
Swati N 2022 Fractional order sir epidemic model with beddington-de angelis incidence and holling type ii treatment rate for covid-19 *J. Appl. Math. & Computing* **68** 1
Taneco-Hernández M A and Vargas-De-León C 2020 Stability and lyapunov functions for systems with atangana-baleanu caputo derivative: an hiv/aids epidemic model *Chaos, Solitons Fractals* **132** 109586
Toufik M and Atangana A 2017 New numerical approximation of fractional derivative with non-local and non-singular kernel: application to chaotic models *The European Physical Journal Plus* **132** 1–16
Wang X 2004 A simple proof of descartes's rule of signs *The American Mathematical Monthly* **111** 525
WHO (2020). Director-Generals opening remarks at the media briefing on COVID-19—11 March 2020 (No. March). Retrieved 2022-08-08, from (https://www.who.int/director-general/speeches/detail/who-director-general-s-opening-remarks-at-the-media-briefing-on-covid-19—11-march-2020)
Yasir K A and Liu W-M 2021 Social distancing mediated generalized model to predict epidemic spread of covid-19 *Nonlinear Dyn.* **106** 1187–95
Yavuz M, Coşar F Ö, Günay F and Özdemir F N 2021 A new mathematical modeling of the covid-19 pandemic including the vaccination campaign *Open Journal of Modelling and Simulation* **9** 299–321
Zhou L and Fan M 2012 Dynamics of an sir epidemic model with limited medical resources revisited *Nonlinear Anal. Real World Appl.* **13** 312–24